JPE 19-3-10

https://doi.org/10.6113/JPE.2019.19.3.714
ISSN(Print): 1598-2092 / ISSN(Online): 2093-4718

Hybrid-Boost Modular Multilevel Converter-Based Medium-Voltage Multiphase Induction Motor Drive for Subsea Applications

Mohamed Daoud[†,*], Ahmed Elserougi[***], Ahmed Massoud[*], Radu Bojoi[**], Ayman Abdel-Khalik[***], and Shehab Ahmed[****]

[*]Department of Electrical Engineering, Qatar University, Doha, Qatar
[†,**]Department of Energy, Polytechnic University of Turin, Turin, Italy
[***]Department of Electrical Engineering, Alexandria University, Alexandria, Egypt
[****]Texas A&M University at Qatar, Education City, Qatar

Abstract

This paper proposes a hybrid-boost Modular Multilevel Converter (MMC) for the Medium-Voltage (MV) Variable Speed Drives (VSDs) employed in subsea applications, such as oil and gas recovery. In the presented architecture, a hybrid-boost MMC with a reduced number of semiconductor devices driving a multiphase Induction Machine (IM) is investigated. The stepped output voltage generated by the MMC reduces or eliminates the filtering requirements. Moreover, the boosting capability of the proposed architecture eliminates the need for bulky low-frequency transformers at the converter output terminals. A detailed illustration of the hybrid-boost MMC operation, the expected limitations/constraints, and the voltage balancing technique are presented. A simulation model of the proposed MV hybrid-boost MMC-based five-phase IM drive has been built to investigate the system performance. Finally, a downscaled prototype has been constructed for experimental verification.

Key words: Five phase, Hybrid boost, Medium voltage, Motor drive, Subsea

I. INTRODUCTION

The subsea industry comprises several operations that are performed at deep sites beneath the water. These operations include exploration, drilling, and oil and gas development. A number of subsea power transmission and distribution topologies, in addition to equipment location scenarios (onshore, offshore, seabed, etc.) were illustrated in [1]. In subsea applications, the electrical drive systems for seabed compressors and pumps are commonly located topside on vessels far from the seabed, with distances of up to 150km [2]. Commonly, these drive systems are operated at Medium-Voltage (MV) levels [3], such as ABB drive systems: ASC 1000 (4.16kV with 5MW), ASC 6000 (3.3kV with 27MW), and PSC 8000 (6.6kV with 100MW).

In these MV high-power drive systems, three main system components should be considered for proper design and operation, namely the power converter, the electric machine, and the transformer (with a shunt passive filter, particularly when considering long feeders).

Conventionally, a drive system containing two-level inverters (2L-Inverter) and a three-phase Permanent Magnet Synchronous Motor (PMSM) or Induction Machine (IM), is used due to its simplicity. However, such a drive system requires: 1) a bulky transformer at the converter output due to the limitations or unavailability of high-voltage switching devices; 2) high switching frequency operation; and 3) a large filter at the converter output [4], as shown in Fig. 1(a).

In order to optimize the technical requirements of the drive system such as the power density (MW/m^3), specific power (MW/kg), and footprint (m^2/MW), a transformerless and

Manuscript received Jun. 30, 2018; accepted Jan. 9, 2019
Recommended for publication by Associate Editor P. Sanjeevikumar.
[†]Corresponding Author: mohamed.daoud@polito.it
Tel: +393917900387, Polytechnic University of Turin
[*]Department of Electrical Engineering, Qatar University, Qatar
[**]Department of Energy, Polytechnic University of Turin, Italy
[***]Department of Electrical Engineering, Alexandria Univ., Egypt
[****]Texas A&M University at Qatar, Qatar

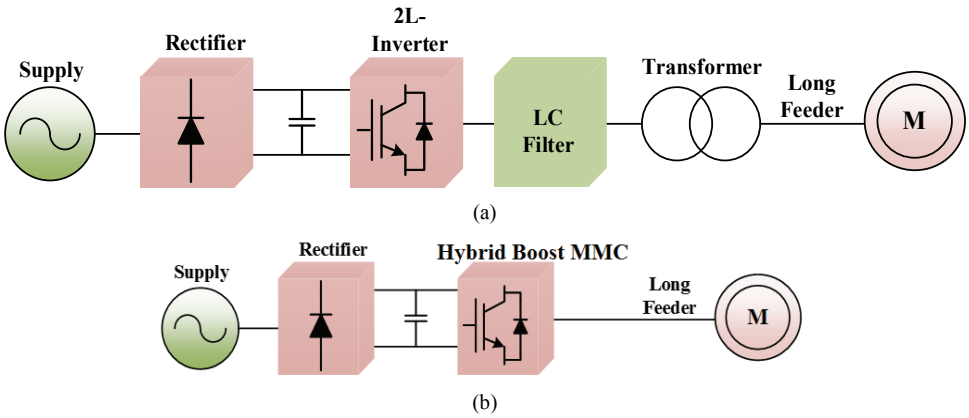

Fig. 1. Conventional and proposed ac drive system structures. (a) Conventional drive. (b) Proposed hybrid-boost-based drive.

filterless operation is targeted. This can be achieved through MV multilevel converters, which enhance the power quality, and reduce the *dv/dt* stresses and Common Mode Voltage (CMV). This enables the deployment of low-voltage semiconductor devices for higher voltage ratings.

Diode-clamped, flying-capacitor and cascaded H-bridge multilevel converters all have challenges, such as the requirements of high numbers of diodes, capacitors and isolated dc sources, which decrease the system power density and specific power. Modular Multilevel Converters (MMCs) overcome the aforementioned challenges, in addition to enhancing power quality, scalability and reliability with fault ride through capability. Moreover, the attainable stepped output voltage results in lower harmonic content and *dv/dt*, which eliminates the need for bulky reactive components (i.e., filters at the converter output terminals). Nonetheless, the main challenge of MMCs in drive system operation is constant torque applications that require a rated torque at a wide range of speeds, including low speeds. It should be noted that Sub-Module (SM) capacitor voltage ripples are inversely proportional to the phase current frequency. The MMC has been thoroughly discussed for medium/high-power motor drive applications in [5]-[11], where several solutions (software-based and/or hardware-based) have been proposed to comply with the requirements of the zero/low-speed operation. On the other hand, the MMC is a suitable candidate for high-power fan, compressor and pump loads, where the torque is proportional to the square of the motor speed [6], [12]. A conventional MMC-based MV three-phase IM drive system was proposed in [13], [14] for high-power applications in the oil and gas industry.

Boost MMCs add a stepping-up capability to converters at the cost of increasing the number of semiconductor devices. This assists in reducing the dc-link voltage, which is a challenge in MV applications during system startup, shutdown, and normal operation. In addition, the bulky low-frequency high-power transformers may be eliminated, as shown in Fig. 1(b).

In a boost MMC, an ac output of kV_{dc} peak, where k is a positive integer and V_{dc} is the input dc-link voltage, can be generated [15]. IN this case, each arm contains $(2k+1)h$ Full-Bridge Sub-Modules (FB-SMs) each rated at $0.5V_{dc}/h$, where h is a positive integer.

The voltage range of upper/lower arms is between $(0.5-k)V_{dc}$ and $(0.5+k)V_{dc}$, which results in a $(4kh+1)$-level ac output voltage with a magnitude of (kV_{dc}). On the other hand, in order to reduce the number of switching devices, a hybrid-boost MMC can be adopted. It contains a combination of $2h$ Half-Bridge SMs (HB-SMs) and $(2k-1)h$ FB-SMs per arm, i.e., a ratio of $(2k-1):2$ for the number of FB-SMs to the number of HB-SMs can be employed, to generate an ac output voltage with a peak of kV_{dc}. For example, with k=2, a ratio of 3:2 should be employed. Meanwhile, when k =1, a ratio of 1:2 is adopted. For the sake of simplicity, the 1:2 hybrid-boost MMC is employed throughout this paper, where an ac output voltage peak of up to V_{dc} can be generated. For higher ac output voltages, other ratios can be adopted in a similar fashion. It is worth noting that operating with the aforementioned ratios results in missing the dc fault blocking capability. However, the dc fault blocking feature in drive systems is not as essential as it is in HVDC systems, since the machines do not contribute to faults in the dc-side.

With the development of power electronics, particularly wide-bandgap devices, enhanced efficiency, specific power, and power density can be achieved with the possibility of an increase in cost [16]. Nevertheless, using high-voltage wide bandgap devices in high-power MV drive system applications is still in the infancy stage. However, off-the-shelf Si semiconductor devices are limited to 6.5kV. The higher the rated voltage of the semiconductor devices, the lower the switching capability together with corresponding higher losses. This highlights the double facet benefits of using MMCs with semiconductor devices of lower voltage ratings both through increasing the switching capability, hence enhanced power quality (i.e., reduced THD), and through reducing the semiconductor devices losses, hence enhanced efficiency. In addition, reducing the semiconductor devices losses affects the required heatsinks, which enhances both the

power density and the specific power. Moreover, reductions in the footprint and cost can be achieved. Increasing the number of cells in MMCs may affect reliability, but has the benefit of providing redundancy [17].

This paper proposes multiphase machines, which reduce the required voltage rating for the same power and phase current, when compared with three-phase based systems. This, in turn, reduces the insulation requirements. Moreover, multiphase machines enhance the reliability, fault ride through capability and power density, in addition to reducing torque ripples [18], [19].

In this paper, a transformerless and filterless ac drive structure for subsea applications is proposed as shown in Fig. 1(b). The proposed structure employs a hybrid-boost MMC along with a five-phase IM, which introduces the following merits.

1. Reduced dc-link voltage, when compared with alternatives based on three-phase machines and/or conventional MMCs.
2. Enhanced efficiency, when compared with alternatives that rely on other multilevel converter topologies.
3. Enhanced power density and specific power, combined with a reduced footprint.
4. Enhanced reliability, with fault ride through capability.

The main contribution of this paper can be summarized as follows.

1. Proposing a multiphase hybrid-boost MMC-based drive system for subsea applications that enables fault tolerant operation.
2. The boosting capability of the proposed MMC enables transformer-less operation in MV drives, since the boosting ratio can reach up to kV_{dc} by increasing the number of FB-SMs. Transformerless operation inherently enhances the drive system performance and reduces its footprint.

This paper consists of six sections. Section I presents the introduction and main contributions. The basics of the conventional MMC and a MMC with boosting capability are presented in section II. Section III elucidates the operational concept and voltage balancing technique of the employed 1:2 hybrid-boost MMC. Section IV assesses the effect of the motor power factor on capacitor voltage balancing. Section V validates the proposed AC drive structure via simulation and experimental results. Finally, Section VI summarizes the contributions of the paper.

II. MMC Basics

A. Conventional HB-SM-Based MMC

HB-SMs and FB-SMs are the most common SMs for MMCs. Conventional HB-SMs-based MMCs have no boosting capability since the peak of the generated ac voltage can be controlled to up to 50% of the input dc voltage, as shown in

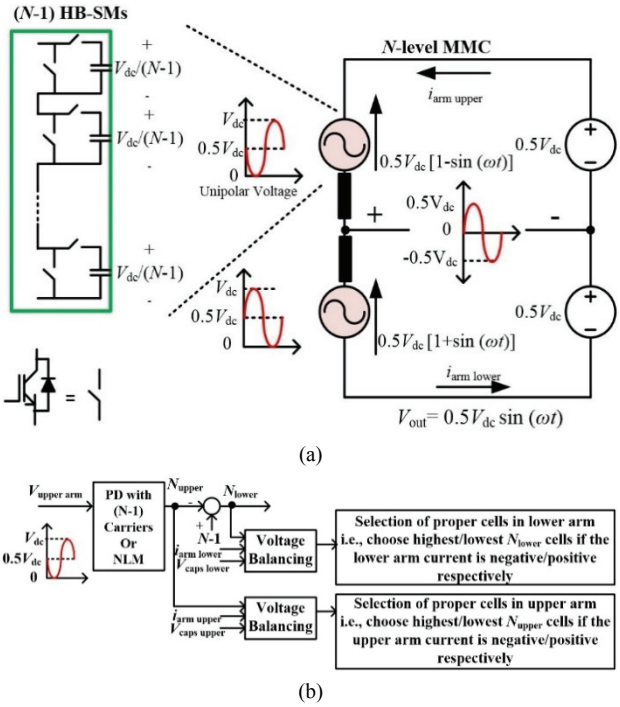

Fig. 2. Per-leg basic operation of a conventional MMC at a unity modulation index ($M=1$). (a) Architecture. (b) Voltage balancing.

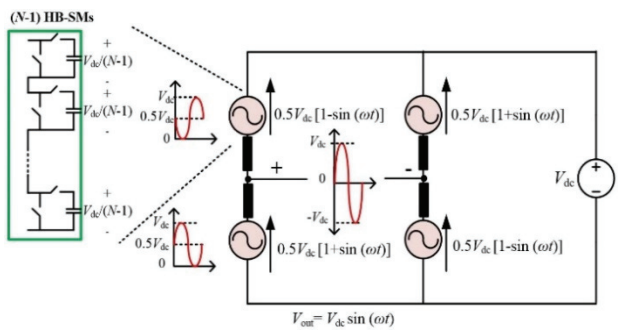

Fig. 3. Single-phase MMC with the H-bridge concept.

Fig. 2. The per-leg operation of the conventional HB-MMC is shown in Fig. 2(a). The capacitor voltages of the SMs should be kept balanced by applying a proper voltage balancing technique such as Phase-Disposition (PD) or Nearest Level Modulation (NLM) techniques [20], [21], as shown in Fig. 2(b).

B. MMC with Voltage Boosting Capability

To have an output voltage peak of up to V_{dc} with HB-SMs, a MMC with two legs per phase can be used (H-bridge concept), as shown in Fig. 3. The voltage balancing technique should be independently applied to each leg as shown in Fig. 2(b). The number of output voltage levels in this configuration mainly depends on the modulation technique. For example, if the PD modulation technique is employed with the configuration shown in Fig. 3, *(2N-1)* voltage levels can be obtained for *(N-1)* HB-SMs per arm. The H-bridge configuration (Fig. 3) can generate a boosted ac output voltage. However, it requires a higher number of arm inductors and capacitors when compared

to the hybrid-boost MMC. It also corresponds to a larger number of semiconductor devices in the case of multiphase systems.

On the other hand, the boost FB-MMC [22] allows for increasing the ac output voltage by 100%, when compared to the conventional HB-SMs-based MMC, by increasing the number of FB-SMs by 50% (i.e., an ac output voltage peak of V_{dc} can be generated). The main disadvantage of the boost FB-MMC is the large number of semiconductor devices, which negatively affects the system cost and losses. To reduce the number of employed semiconductor devices, hybrid MMCs have been proposed with different ratios of FB-SMs and HB-SMs per arm, where 1:1 and 2:1 ratios have been presented in [15] and [23], respectively.

The 1:1 hybrid MMC has no boosting capability. On the other hand, the 2:1 hybrid MMC [15] can be considered as a proper replacement for the boost FB-MMC since it maintains both boosting and dc fault blocking capability with a lower number of semiconductor devices. As a further reduction for the employed semiconductor devices, while maintaining the boosting capability, a 1:2 hybrid-boost MMC with a combination of FB-SMs and HB-SMs with a ratio of 1:2 per arm has been proposed in [24]. The total number of SMs per arm in the 1:2 hybrid-boost MMC is *3(N-1)/4*, where *N* is the number of output voltage levels. In this case, the SMs are rated at $2V_{dc}/(N-1)$. The 1:2 hybrid-boost MMC can increase the utilization of the dc input voltage by 100%, i.e., the peak of the ac output voltage can be controlled up to V_{dc} (i.e., boosting capability).

The main drawback of the 1:2 hybrid-boost MMC configuration is that it has no dc fault blocking capability. However, this is a less significant feature in ac motor drives when compared with HVDC systems.

Generally, in order to generate higher ac output voltages (up to kV_{dc}), a hybrid-boost MMC, which contains a combination of *2h* HB-SMs and *(2k-1)h* FB-SMs per arm each rated at $0.5V_{dc}/h$, can be employed [25]. In this paper, a 1:2 hybrid-boost MMC is considered for the sake of simplicity (i.e., k=1). The same concept can be applied for higher ac output voltages (i.e., k>1). However, it uses other ratios according to the aforementioned rule.

III. Operational Concepts of the 1:2 Hybrid-Boost MMC

A. Architecture

Unlike HB-SMs, FB-SMs are able to generate a negative voltage as shown in Fig. 4. The 1:2 hybrid-boost MMC (i.e. k=1) is shown in Fig. 5. Each arm of the *N*-level hybrid-boost MMC consists of *(N-1)/2* HB-SMs and *(N-1)/4* FB-SMs, where *N=4h+1*. The capacitors for all of the SMs are pre-charged to a $0.5V_{dc}/h$ voltage level.

In the 1:2 hybrid-boost MMC, the arm voltage is controlled

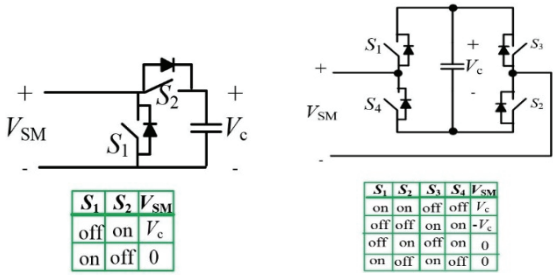

Fig. 4. Output voltage states. (a) HB-SM. (b) FB-SM.

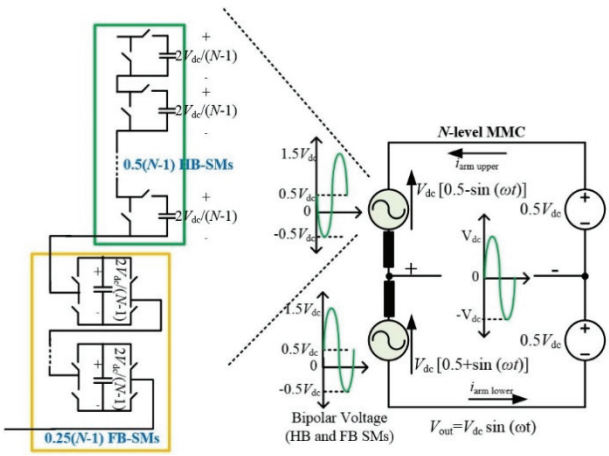

Fig. 5. One-phase of the 1:2 hybrid-boost MMC.

to generate a bipolar voltage ranging from $-0.5V_{dc}$ to $+1.5V_{dc}$ (at the highest possible output) as shown in Fig. 5. This in turn, enables controlling the peak of the generated ac voltage up to V_{dc}. During the generation of the positive part of the arm voltage, both HB-SMs and FB-SMs are used.

The decision of which of these SMs should be activated is the responsibility of the voltage balancing algorithm, which is described in the next section. On the other hand, during the generation of the negative part of the arm voltage, only FB-SMs are used to generate negative SM voltage. Meanwhile, based on the arm current direction and the arm voltage level, a certain number of these FB-SMs is activated.

B. Voltage Balancing Technique

A sensor-based per-leg voltage balancing technique for the hybrid-boost MMC is shown in Fig. 6. A sensorless balancing technique was proposed in [26]. The procedures of the voltage balancing technique for each leg of the 1:2 hybrid-boost MMC are summarized in the following points.

- The reference of the upper arm voltage should be defined so that it is equal to V_{dc} [0.5-α sin ($\omega t+\theta_v$)], where α ranges from $0 < \alpha < 1$, ω is the angular frequency (rad/s), and θ_v is the phase angle of the ac component of the arm voltage.
- The aforementioned voltage reference is added to a dc offset of $0.5V_{dc}$ to generate a unipolar reference voltage (V_x).

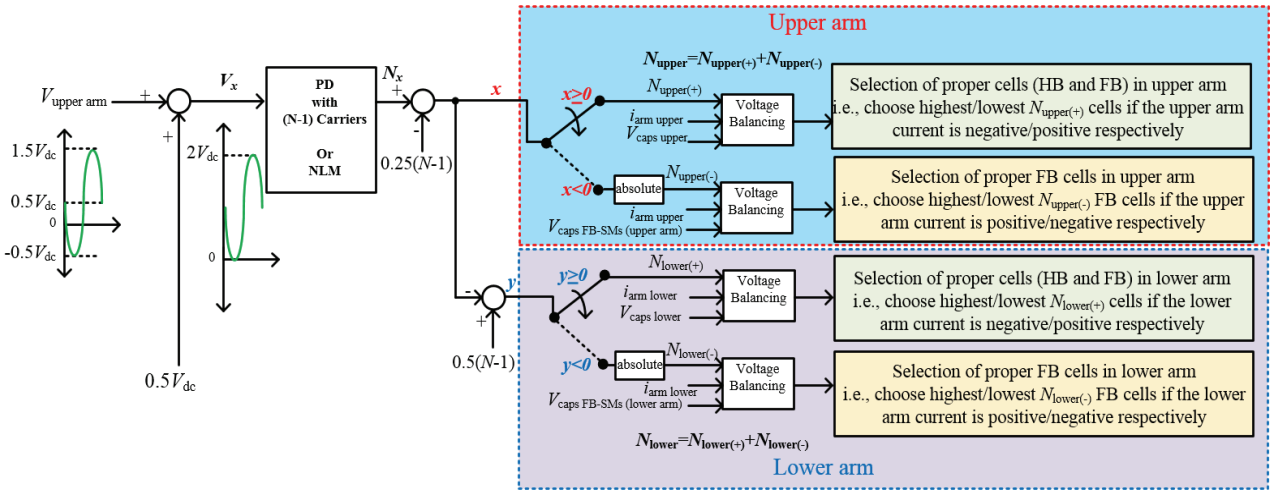

Fig. 6. Per-leg voltage balancing technique of the 1:2 hybrid-boost MMC architecture.

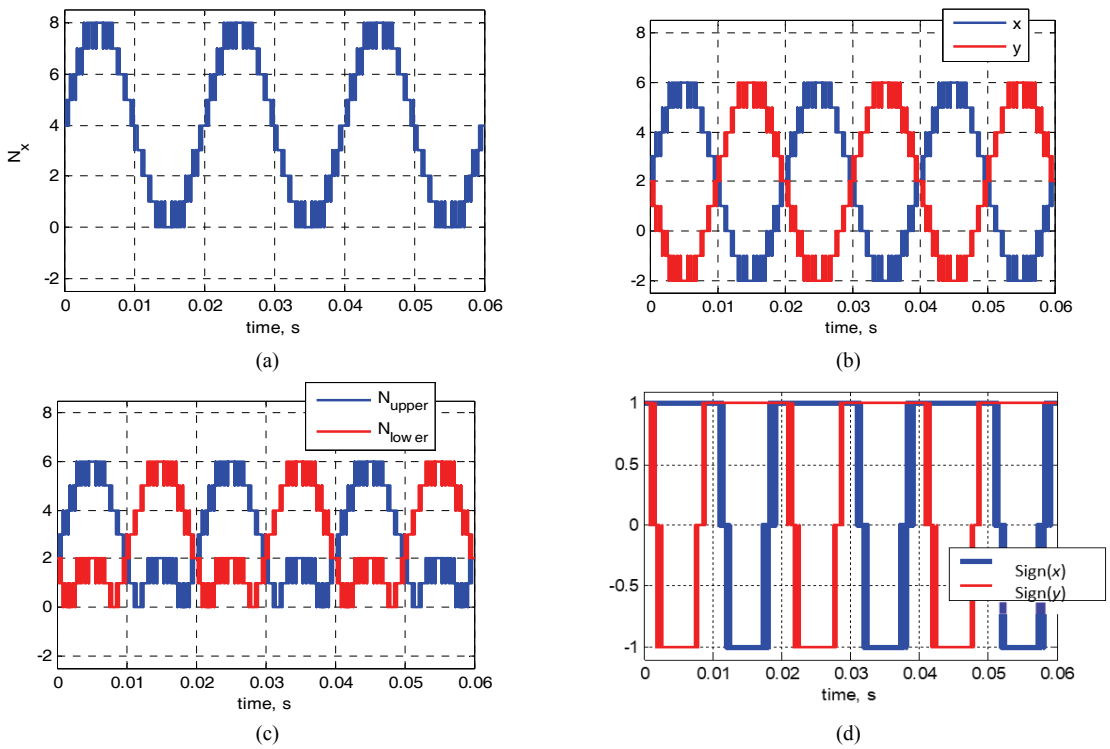

Fig. 7. Illustrations of the voltage balancing procedures. (a) The signal N_x. (b) The signals x and y. (c) The number of SMs involved in the upper and lower arms. (d) The signals sign(x) and sign(y).

- The obtained unipolar reference voltage (V_x) is used to generate a signal, namely N_x, using a carrier-based pulse width modulation technique such as PD shown as in Fig. 7(a), where $\alpha = 1$, $\theta_v = 0$, switching frequency = 2 kHz, $N = 9$, and N_x ranges from 0 to *(N-1)*.
- Then the signal (N_x) can be used to extract two new variables (x and y) as shown in Fig. 7(b), where $x = N_x - 0.25(N\text{-}1)$, while $y = 0.75(N\text{-}1) - N_x$.
- The absolute values of x and y represent the number of SMs to be activated in the upper and lower arms namely, N_{upper} and N_{lower} as shown in Fig. 7(c). The signs of x and y represent the output voltage signs of the activated SMs in upper and lower arms, as shown in Fig. 7(d).
- For a positive x, both HB-SMs and FB-SMs in the upper arm are used to generate the positive part of the upper arm voltage, i.e., the highest/lowest $N_{upper(+)}$ (= x) SMs will be selected, if the upper arm current is negative/positive, respectively.
- For a negative x, only FB-SMs in the upper arm are used to generate the negative part of the upper arm voltage,

i.e., the highest/lowest $N_{upper(-)}$ (= $|x|$) FB-SMs will be selected, if the upper arm current is positive/negative, respectively.

- For a positive y, both HB-SMs and FB-SMs in the lower arm are used to generate the positive part of the lower arm voltage, i.e., the highest/lowest $N_{lower(+)}$ (= y) SMs will be selected, if the upper arm current is negative/ positive, respectively.
- For a negative y, only FB-SMs in the lower arm are used to generate the negative part of the lower arm voltage. i.e., the highest/lowest $N_{lower(-)}$ (= $|y|$) FB-SMs will be selected, if the lower arm current is positive/negative, respectively.

IV. Effect of the Five-Phase Motor Power Factor on Capacitor Voltages Balancing

Assuming an ideal five-phase converter, the average dc-side and ac-side powers in the proposed approach are given by $P_{dc}=I_{dc}\ V_{dc}$ and $P_{ac}= 5\ I_m\ V_m \cos(\phi)/2$, where V_{dc} is the input dc voltage, I_{dc} is the average of the input dc current, and I_m and V_m are the peak of the load phase current and voltage, respectively. Meanwhile, cos (ϕ) is the motor power factor, and the voltage of phase "A" is $v_{ph}(t) = V_m \sin(\omega t)$. By equating the two powers and substituting with $V_m=V_{dc}$ (i.e., assuming the highest output voltage in the proposed structure), the average of the input dc current can be expressed by:

$$I_{dc} = 2.5\ I_m \cos(\phi) \tag{1}$$

The following analysis is presented for the upper arm. Similar procedures can be applied to the lower arm. If the circulating currents are well-suppressed, the upper arm current of phase "A" can be expressed by:

$$i_{arm\ upper}(t) = 0.5\ i_{ph}(t) + 0.2\ I_{dc} \tag{2}$$

Substituting (1) into (2) yields:

$$i_{arm\ upper}(t) = 0.5\ I_m [\cos\phi + \sin(\omega t - \phi)] \tag{3}$$

The corresponding upper arm voltage reference of phase "A" can be expressed by:

$$v_{arm\ upper}(t) = 0.5 V_{dc} - V_m \sin(\omega t) \tag{4}$$

which ranges from $-0.5V_{dc}$ to $+1.5V_{dc}$. When $-0.5V_{dc} \leq v_{arm\ upper}(t) \leq 0$, FB-SMs are only operated to generate the negative output voltage state. Meanwhile, the arm current direction determines the charging/discharging of the FB-SMs capacitors for the negative or positive upper arm currents, respectively. Furthermore, when $0 \leq v_{arm\ upper}(t) \leq 1.5V_{dc}$, adequate SMs from HB-SMs and/or FB-SMs are operated based on the balancing algorithm to generate the positive output state.

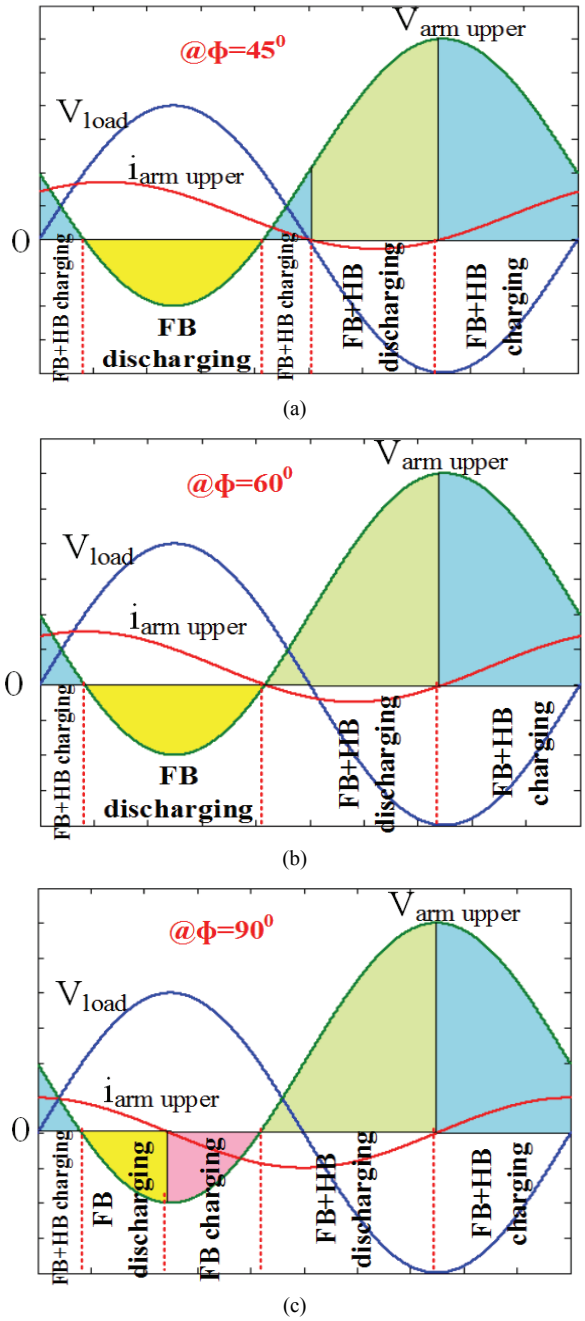

Fig. 8. Illustrations of the effect of the load power factor on the charging and discharging periods of SMs capacitors. (a) ϕ=45º. (b) ϕ=60º. (c) ϕ=90º.

Similarly, the arm current direction determines the charging/ discharging of the HB-SMs and/or FB-SMs capacitors. Variations of the upper arm current and voltage during a complete fundamental cycle for different load power factors, along with an illustration of the charging and discharging periods of FB-SMs and HB-SMs with the operation are shown in Fig. 8. It is clear that as the load angle increases, the area of the negative upper arm current increases, which increases the possible time for discharging HB-SMs. In case of a low negative upper arm current area, the discharging

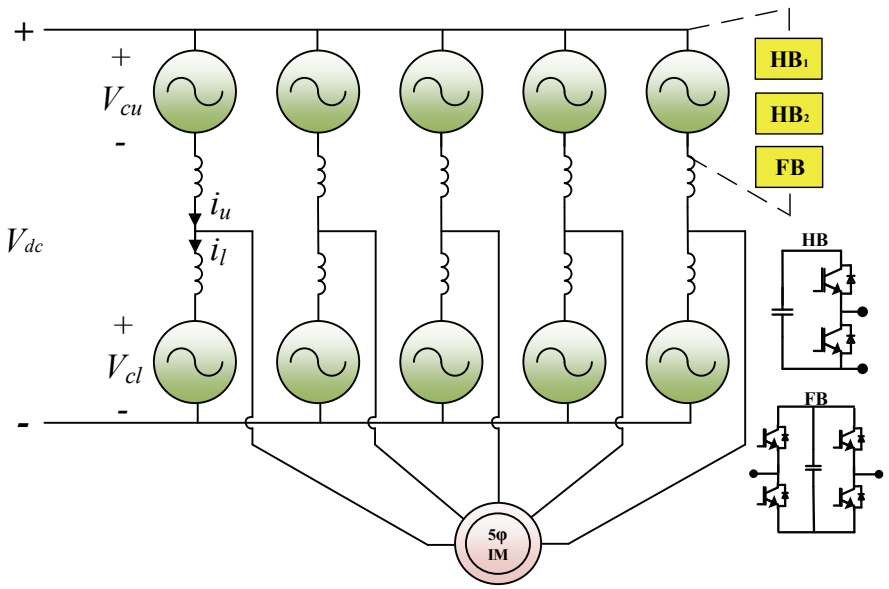

Fig. 9. 1:2 hybrid-boost MMC-based multiphase IM drive system, where *u* and *l* refer to the upper and lower arms, respectively.

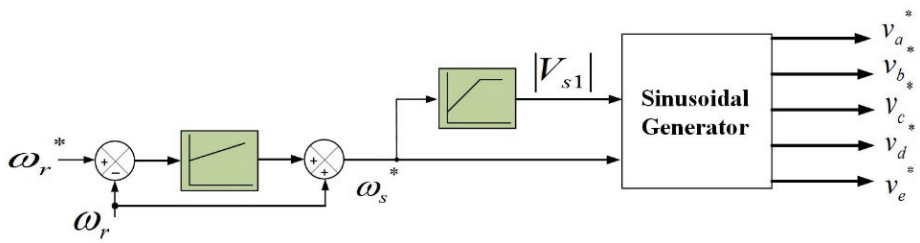

Fig. 10. Block diagram of the *V/f* control, where ω_r is the motor speed, ω_s is the flux synchronous speed, and V_{s1} is the fundamental component of the stator voltage.

time interval for HB-SMs is insufficient, which results in a mismatch in the voltages of the FB-SMs and HB-SMs.

V. Performance of the 1:2 Hybrid-Boost MMC-Based Medium-Voltage Five-Phase Induction Motor Drive

In MV applications, such as subsea oil and gas recovery, MMCs, such as high-power converters, have a good potential to be deployed in pump applications, particularly with the advantageous torque-speed characteristics of the pump loads in terms of the MMC operation. The configuration of the proposed drive system is shown in Fig. 9. Referring to Fig. 5 in the presented case study, a five-level five-phase 1:2 hybrid-boost MMC with (N=5, k=1 and h=1) is used to feed a five-phase IM.

In the presented case study, the employed five-phase hybrid-boost MMC contains 80 switching devices distributed as 4 HB-SMs and 2 FB-SMs per phase (upper and lower arms). The voltage balancing technique, in Section III. B, is utilized for each leg of the converters to ensure successful operation with balanced capacitors voltages. Meanwhile, the five-phase IM fosters system reliability and fault tolerance.

In the following subsections, simulation and experimental results are presented, where a simulation model of a 1:2 hybrid-boost MMC-based MV multiphase drive is built to test the converter performance. Meanwhile a scaled-down 1:2 hybrid-boost MMC is implemented for experimental validation.

A. System Simulation

In this section, the drive system performance during steady-state operation is investigated using MATLAB/Simulink. *V/f* scalar control, shown in Fig. 10, is used to drive the machine at the rated operating conditions. A simulation model for a 1:2 hybrid-boost MMC-based MV drive with a 1000 hp five-phase distributed winding IM has been built with the parameters shown in Table I.

The model equations of a five-phase IM can be found in [27]. Based on the data shown in Table I, to generate the IM rated phase voltage (peak=3.394 kV) from the 1:2 hybrid-boost MMC, a dc-link voltage of 3.4 kV is employed. The machine is started under no-load at t = 0. Then a load torque is applied at t = 1s. The simulation results are shown in Fig. 11, assuming a 2 kHz carrier switching frequency. The machine planes are mapped into two main orthogonal frames (the α-β frame and the x-y frame) in addition to the zero-sequence frame. The α-β

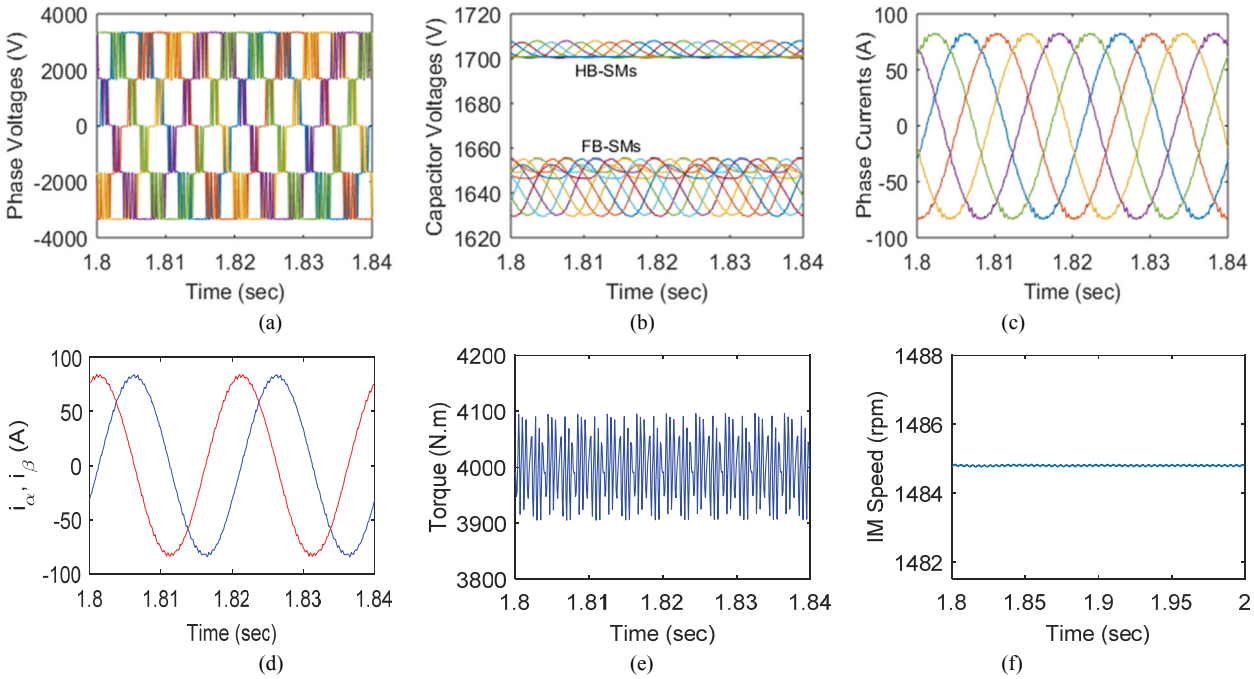

Fig. 11. Simulation results under steady-state operation. (a) MMC output phase-to-midpoint voltages. (b) Capacitor voltages. (c) Machine phase currents. (d) Fundamental $\alpha\beta$ currents. (e) Machine torque. (f) Machine speed.

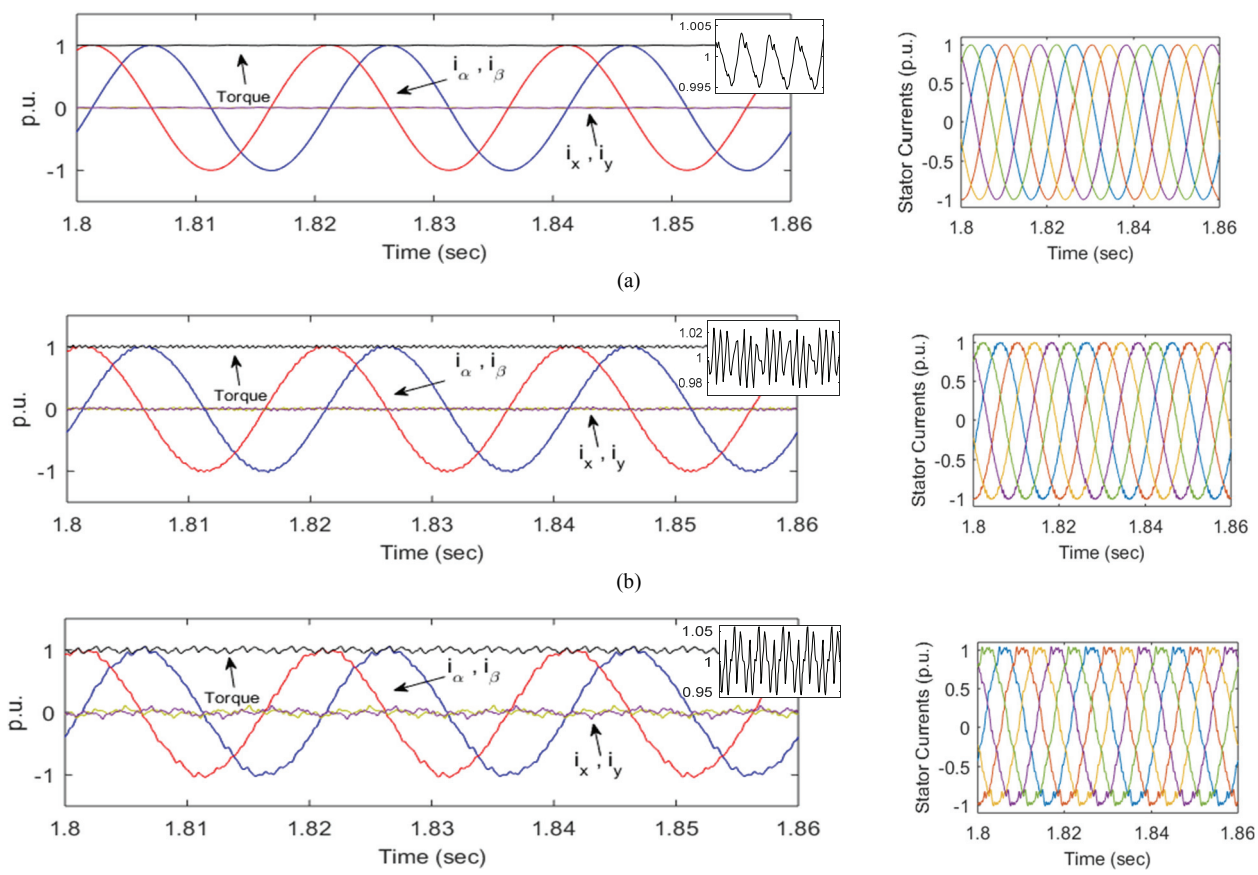

Fig. 12. Effect of the carrier frequency on the stator currents and the delivered torque ripples (per-unit values). (a) f_s=10 kHz. (b) f_s=2 kHz. (c) f_s=1 kHz.

TABLE I
SIMULATION PARAMETERS

DC-link voltage (kV)	3.4	IM rated torque (N.m)	4000
IM rated phase voltage (kV)	2.4	IM stator resistance (Ω)	0.5148
IM rated power (Hp)	1000	IM stator leakage reactance (Ω)	3.33
Fundamental frequency (Hz)	50	IM rotor referred resistance(Ω)	0.4116
No. of poles	4	IM rotor referred reactance (Ω)	2.7
FB-/HB-SM's capacitor (mF)	1	Magnetizing reactance (Ω)	163

frame represents the electromechanical energy conversion, while the *x-y* frame represents the harmonics/losses plane.

Fig. 11(a) shows the delivered phase-to-midpoint voltages, which have a peak value equal to the input dc voltage (V_{dc}). With $N = 5$, i.e. h=1, in the simulated 1:2 hybrid-boost MMC, the output voltage consists of five different voltage levels (-1, -0.5, 0, 0.5 and 1) V_{dc}. Fig. 11(b) shows that the capacitor voltages are balanced at around $0.5V_{dc}$ (generally, $2V_{dc}/(N\text{-}1)$ as in Fig. 5). The difference between the FB-SMs and HB-SMs voltages is caused by the unequal charging/discharging times of both modules depending on the load power factor, as illustrated in section IV and Fig. 8. The stator phase currents are balanced and identical as shown in Fig. 11(c). In addition, $i_{s\alpha}$ and $i_{s\beta}$, which are responsible for torque production, are shown in Fig. 11(d). The output torque is shown in Fig. 11(e), which exhibits a percentage torque ripple of only 2.25% at a relatively low switching frequency. Fig. 11(f) shows the machine speed. Even though the MMC eases the low switching frequency operation, the torque ripples remain a concern for drive systems.

Fig. 12 shows a torque ripple profile at different switching frequencies to conclude a range for the minimum permissible operating switching frequency that yields an acceptable percentage of torque ripple. The output torque ripple magnitude changes by changing the frequency of the carrier responsible for assigning the number of required upper and lower SMs.

Fig. 12 shows the output phase currents, current components and the corresponding delivered torque at different switching frequencies. With a carrier frequency of 10 kHz, the output current has the lowest harmonics with the lowest i_{sx} and i_{sy} components and torque ripples being barely 1%. For a carrier frequency of 2 kHz, the ripples in the $i_{s\alpha}$ and $i_{s\beta}$ components increase to 1.7%, which affects the torque.

However, the torque ripples are still acceptable at 2.25%. When the carrier frequency is dropped to 1 kHz, the stator currents are more distorted, as shown in Fig. 11(c), which can be deduced from the i_{sx} and i_{sy} components. The current THD is increased to 8.3%. However, the torque ripples are just 3% due to the lower presence of harmonics in the torque producing components $i_{s\alpha}$ and $i_{s\beta}$. The THD currents and torque ripples

TABLE II
TORQUE RIPPLES AND THDS WITH SWITCHING FREQUENCY CHANGES

	f_s= 0.5 kHz	f_s=1 kHz	f_s=2 kHz	f_s=10 kHz
Torque ripples %	14.6	3	2.25	0.4
THD phase currents %	17.68	7.6	2.4	0.8
THD $\alpha\beta$ currents %	10.7	3.4	1.7	0.37

TABLE III
EXPERIMENTAL SETUP PARAMETERS

SM's capacitor voltage rating (V)	350	DC-link applied voltage (V)	200
FB-/HB-SM's capacitor (μF)	470	IGBT IKW75N60T rating	30A/1200V
Arm inductor (mH)	0.5	Switching frequency (Hz)	1000

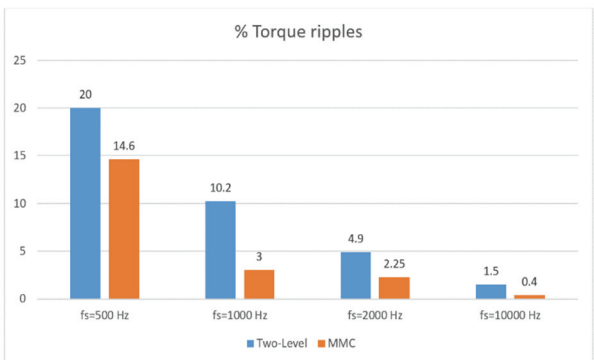

Fig. 13. Generated ripples in the output torque of the hybrid-boost MMC vs. a conventional 2-Level inverter with changes in the switching frequency.

at different switching frequencies are summarized in Table II. It is worth noting that the torque ripples are significantly less than the ripples when the simulation was performed using a conventional five-phase two-level converter, as shown in Fig. 13.

B. Experimental Validation

A downscaled experimental single-phase prototype was built to validate the proposed topology. For the sake of simplicity, a single-phase 5-level 1:2 hybrid-boost MMC was applied to a single-phase inductive load with a low inductance value, since the experiment was performed under the worst-case scenario for capacitor voltage balancing of approximately a unity power factor.

Fig. 14(a) shows a schematic diagram of the experimental rig, where the capacitor voltages and arms currents are measured and then fed to a Digital Signal Processor (DSP) to perform the aforementioned suggested voltage balancing technique (Fig. 6) for the given output voltage reference. Fig. 14(b) shows the implemented experimental rig. Table III shows the experimental setup specifications.

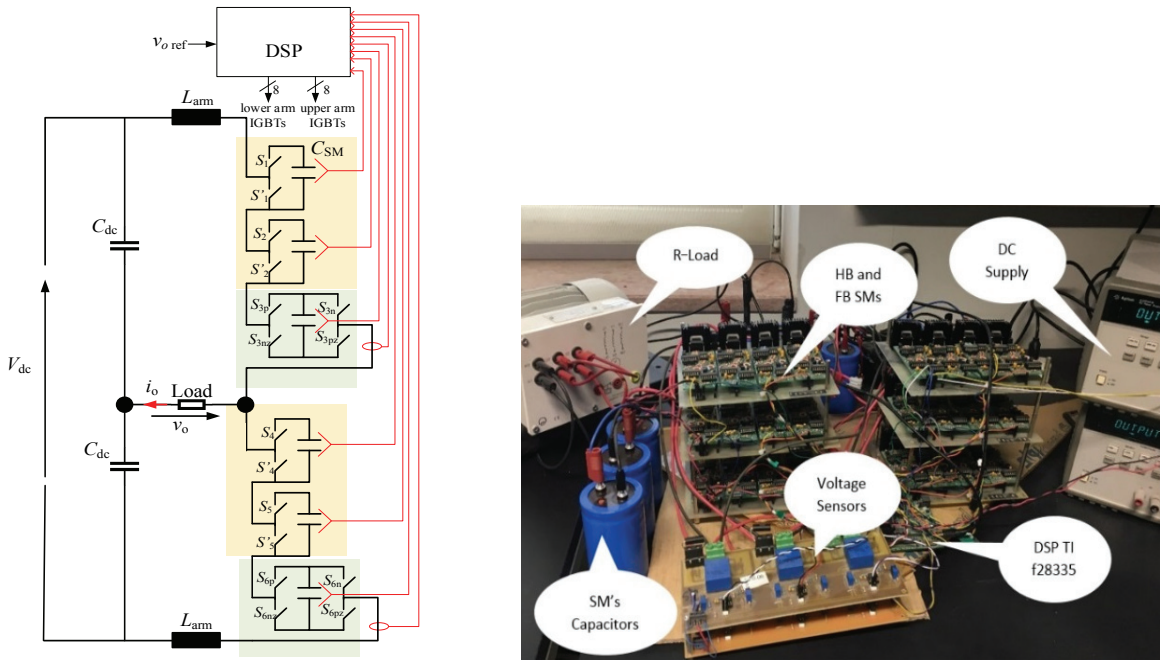

(a) (b)

Fig. 14. Experimental validation. (a) Schematic diagram. (b) Experimental rig.

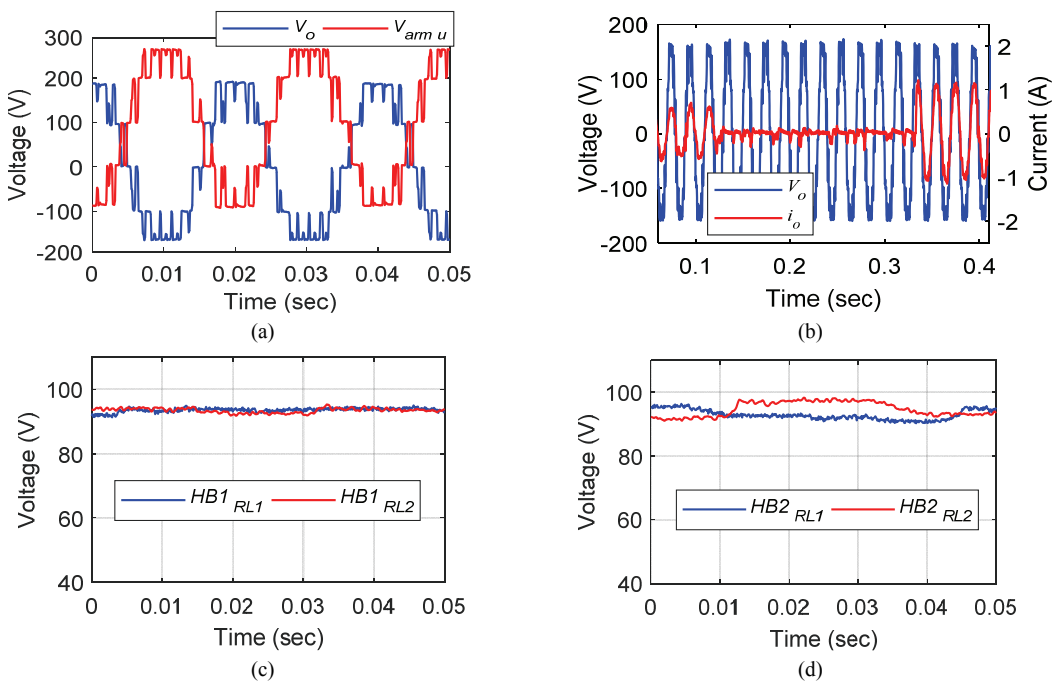

Fig. 15. Experimental results. (a) Output and upper arm voltages. (b) Output voltage and current with load changes. (c) Capacitor voltage of HB_1. (d) Capacitor voltage of HB_2 at two different loading conditions R_{L1}=290Ω and R_{L2}=155Ω.

The obtained experimental results are shown in Fig. 15 where the PD technique is used to generate the number of SMs to be included in each arm. As shown in Fig. 15(a), the 1:2 hybrid-boost MMC delivers an output voltage of 5-levels with a peak value that is approximately equal to the dc-link input, with a voltage drop due to the on-state resistance/voltage of the applied IGBTs. The upper arm voltage is shown in Fig. 15(a). It is clear that it consists of four levels of five different voltage levels (-0.5, 0, 0.5, 1, 1.5) V_{dc}. The output voltage and current, when the load is changed from R_{L1}=290Ω to open circuit to R_{L2}=155Ω, is shown in Fig. 15(b). The current magnitude at a 290Ω load is approximately 0.6 A, while it is equal to 1.1 A at 155Ω.

The capacitor voltages of two different HBs, namely HB_1 and

HB_2, are shown in Figs. 15(c) and 15(d) with the loading changed from R_{L1} to R_{L2}, respectively. The capacitor voltages are balanced in both cases and fluctuate around $0.5V_{dc}$. The obtained experimental results support the proposed topology where an MMC with boosting capability is validated with a reduced number of FBs.

VI. CONCLUSION

This paper introduced a VSD system based on a hybrid-boost MMC accompanied with a 5-phase IM as an alternative to the bulky drive systems used in MV subsea applications. Generally, a stepped ac output voltage with a peak of up to kV_{dc}, where $k > 1$, can be obtained at the output terminals of the ($2k$-1):2 hybrid-boost MMC with a reduced number of semiconductor devices when compared to existing boost MMC configurations. Having a boosting capability results in eliminating the bulky low-frequency step-up transformer. In the presented case study, a hybrid-boost MMC, which contains a combination of FB-SMs and HB-SMs with a ratio of 1:2, is employed. The hybrid-boost MMC is able to deliver an ac output voltage magnitude that is twice the voltage of other medium-voltage MV converters including the conventional MMC (i.e., k=1). The high output quality also eliminates the need for the filtering stage at the output side. In addition, the multiphase machine enhances the drive system fault tolerance capability and reduces the torque ripple at a relatively low switching frequency, which are critical needs for MV applications. The presented drive system exhibited a good performance with low current THD and torque ripples at a relatively low switching frequency of 2 kHz. The SMs capacitors were balanced with the presented voltage balancing technique. The proposed system was investigated in simulation using MATLAB/Simulink. Then the performance of the 1:2 hybrid-boost MMC was experimentally tested on a downscaled prototype. The obtained experimental results combined with the simulation study demonstrate the good potential for the converter.

ACKNOWLEDGMENT

This publication was made possible by GSRA grant 2-1-0609-14027 from the Qatar National Research Fund (a member of Qatar Foundation).

REFERENCES

[1] K. Rajashekara, H. S. Krishnamoorthy, and B. S. Naik, "Electrification of subsea systems: Requirements and challenges in power distribution and conversion," *CPSS Trans. Power Electron. Apps.*, Vol. 2, No. 4, pp. 259-266, Dec. 2017.

[2] ABB Oil, Gas and Chemicals, *INSUBSEA Power and Automation: Expanding Capacity, Extending Lifespan and Reducing Cost for Oil and Gas Fields*, 2017.

[3] ABB Oil, Gas and Chemicals, *ABB Drives in Chemical, Oil and Gas: Medium Voltage Drives for Greater Profitability and Performance*, 2011.

[4] H. Abu-Rub, J. Holtz, J. Rodriguez, and G. Baoming, "Medium-voltage multilevel converters – State of the art, challenges, and requirements in industrial applications," *IEEE Trans. Ind. Electron.*, Vol. 57, No. 8, pp. 2581-2596, Aug. 2010.

[5] B. Li, S. Zhou, D. Xu, S. J. Finney, and B. W. Williams, "A hybrid modular multilevel converter for medium-voltage variable-speed motor drives," *IEEE Trans. Power Electron.*, Vol. 32, No. 6, pp. 4619-4630, Jun. 2017.

[6] M. Hagiwara, K. Nishimura, and H. Akagi, "A medium-voltage motor drive with a modular multilevel PWM inverter," *IEEE Trans. Power Electron.*, Vol. 25, No. 7, pp. 1786-1799, Jul. 2010.

[7] S. Debnath, J. Qin, and M. Saeedifard, "Control and stability analysis of modular multilevel converter under low-frequency operation," *IEEE Trans. Ind. Electron.*, Vol. 62, No. 9, pp. 5329-5339, Sep. 2015.

[8] B. Li, S. Zhou, D. Xu, R. Yang, D. Xu, C. Buccella, and C. Cecati, "An improved circulating current injection method for modular multilevel converters in variable-speed drives," *IEEE Trans. Ind. Electron.*, Vol. 63, No. 11, pp. 7215-7225, Nov. 2016.

[9] A. Antonopoulos, L. Angquist, L. Harnefors, and H. Nee, "Optimal selection of the average capacitor voltage for variable-speed drives with modular multilevel converters," *IEEE Trans. Power Electron.*, Vol. 30, No. 1, pp. 227-234, Jan. 2015.

[10] B. Tai, C. Gao, X. Liu, and Z. Chen, "A novel flexible capacitor voltage control strategy for variable-speed drives with modular multilevel converters," *IEEE Trans. Power Electron.*, Vol. 32, No. 1, pp. 128-141, Jan. 2017.

[11] Y. S. Kumar and G. Poddar, "Medium-voltage vector control induction motor drive at zero frequency using modular multilevel converter," *IEEE Trans. Ind. Electron*., Vol. 65, No. 1, pp. 125-132, Jan. 2018.

[12] H. Akagi, "Classification, terminology, and application of the modular multilevel cascade converter (MMCC)," *IEEE Trans. Power Electron.*, Vol. 26, No. 11, pp. 3119-3130, Nov. 2011.

[13] D. Krug, S. Busse, and M. Beuermann, "Complete performance test of MV drive with modular multilevel topology for high power oil & gas applications," in *Proc. Petroleum and Chemical Industry Technical Conference (PCIC),* pp. 1-6, 2016.

[14] S. Demmig, J. Andrews, and R.-D. Klug, "Control of subsea motors on multi-km cable lengths by Variable Frequency Drives," in *Proc. Petroleum and Chemical Industry Conference Europe Electrical and Instrumentation Applications*, pp. 1-10, 2011.

[15] R. Zeng, L. Xu, L. Yao, and B. W. Williams, "Design and operation of a hybrid modular multilevel converter," *IEEE Trans. Power Electron*., Vol. 30, No. 3, pp. 1137-1146, Mar. 2015.

[16] T. Nakanishi and J. I. Itoh, "High power density design for a modular multilevel converter with an H-bridge cell based on a volume evaluation of each component," *IEEE Trans. Power Electron.,* Vol. 33, No. 3, pp. 1967-1984, Mar. 2018.

[17] J. E. Huber and J. W. Kolar, "Optimum number of cascaded cells for high-power medium-voltage multilevel converters," in *Proc. IEEE Energy Convers. Congr. Expo*., pp. 359-366, Sep. 2013.

[18] E. Levi, "Advances in converter control and innovative exploitation of additional degrees of freedom for multiphase machines," *IEEE Trans. Ind. Electron.*, Vol. 63, No. 1, pp. 433-448, Jan. 2016.

[19] M. I. Daoud, A. Massoud, A. Abdel-Khalik, and S. Ahmed, "An asymmetrical six-phase induction machine-based flywheel energy storage system using modular multilevel converters," in *Proc. International Conference on Electrical Machines and Systems (ICEMS),* pp. 1-6, 2016.

[20] Maryam Saeedifard, and R. Iravani, "Dynamic performance of a modular multilevel back-to-back HVDC system," *IEEE Trans. Power Del.*, Vol. 25, No. 4, pp. 2903-2912, Oct. 2010.

[21] L. G. Franquelo, J. Rodriguez, J. I. Leon, S. Kouro, R. Portillo, and M. A. M. Prats, "The age of multilevel converters arrives," *IEEE Ind. Electron. Mag.*, Vol. 2, No. 2, pp. 28-39, Jun. 2008.

[22] R. Zeng, L. Xu, L. Yao, and D. J. Morrow, "Precharging and DC fault ride-through of hybrid MMC-based HVDC systems," *IEEE Trans. Power Del.*, Vol. 30, No. 3, pp. 1298-1306, Jun. 2015.

[23] G. P. Adam, K. H. Ahmed, and B. W. Williams, "Mixed cells modular multilevel converter," in *Proc. IEEE Int. Symp. Ind. Electron.*, 2014.

[24] A. Elserougi, A. Massoud, and S. Ahmed, "A transformerless STATCOM based on a hybrid boost modular multilevel converter with reduced number of switches," *Electric Power Systems Research*, Vol. 146, pp. 341-348, 2017.

[25] A. Elserougi, A. Massoud, and S. Ahmed, "Power control of grid-connected high-gain boost full-bridge modular multilevel converter," in *Proc. IEEE Southern Power Electronics Conference (SPEC)*, pp. 1-5, 2017.

[26] M. Daoud, A. Massoud, A. Elserougi, A. S. Abdel-Khalik, and S. Ahmed, "Sensor-less operation of hybrid boost modular multilevel converter for subsea multiphase medium voltage drives," in *Proc. IEEE Southern Power Electronics Conference (SPEC)*, pp. 1-5, 2017.

[27] I. González-Prieto, M. J. Duran, N. Rios-Garcia, F. Barrero, and C. Martín, "Open-switch fault detection in five-phase induction motor drives using model predictive control," *IEEE Trans. Ind. Electron.,* Vol. 65, No. 4, pp. 3045-3055, Apr. 2018.

Mohamed Daoud (M'14) received his B.S. and M.S. degrees in Electrical Engineering from Alexandria University, Alexandria, Egypt, in 2009 and 2013, respectively. He is presently working toward his Ph.D. degree in Electrical Engineering both at the Politecnico di Torino, Turin, Italy and at Qatar University, Doha, Qatar. His current research interests include energy conversion, renewable energy, energy storage systems, electric machines and drives. Mr. Daoud received a best presentation award in the Electric Traction Drives for Road Vehicles session at IEEE IECON'2013.

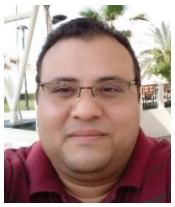

Ahmed Elserougi (SM'13) was born in September 1982, in Alexandria, Egypt. He received his B.S., M.S. and Ph.D. degrees in Electrical Engineering from the Faculty of Engineering, Alexandria University, Alexandria, Egypt, in 2004, 2006 and 2011, respectively. He is presently working as an Associate Professor in the Department of Electrical Engineering, Faculty of Engineering, Alexandria University. His current research interests include power quality, HVDC and FACTS devices, renewable energy, electric power utilities and pulsed power applications.

Ahmed Massoud (SM'11) received his B.S. (first class honors) and M.S. degrees in Electrical Engineering from Alexandria University, Alexandria, Egypt, in 1997 and 2000, respectively. He received his Ph.D. degree in Electrical Engineering from Heriot-Watt University, Edinburgh, SCT, UK, in 2004. He is presently working as a Professor in the Department of Electrical Engineering, College of Engineering, Qatar University, Doha, Qatar. His current research interests include power electronics, energy conversion, renewable energy and power quality. He holds five U.S. patents. He has published more than 100 journal papers in the fields of power electronics, energy conversion and power quality.

Radu Bojoi (F'19) received his M.S. degree in Electrical Engineering from the Technical University of Iasi, Iaşi, Romania, in 1993; and his Ph.D. in Electrical Engineering from the Politecnico di Torino, Turin, Italy, in 2002. He is presently working as a Professor of Power Electronics and Electrical Drives and as the Director of the Power Electronics Innovation Center at the Politecnico di Torino. Dr. Bojoi has published more than 150 papers in the fields of power electronics and electrical drives for industrial applications, transportation electrification, power quality and home appliances. He has been involved in a lot of research projects in the industry for direct technology transfer aiming at obtaining new products. Dr. Bojoi was a co-recipient of 5 prize paper awards, the last one in 2015 was an IEEE-IAS Prize Paper Award. Dr. Bojoi is an Associate Editor of the IEEE Transactions on Industrial Electronics.

Ayman Abdel-khalik (SM'12) received his B.S. and M.S. degrees in Electrical Engineering from Alexandria University, Alexandria, Egypt, in 2001 and 2004, respectively. He received his Ph.D. degree in Electrical Engineering from both Alexandria University and Strathclyde University, Glasgow, SCT, UK, in 2009, under a dual channel program. He is presently working as an Associate Professor in the Department of Electrical Engineering, Faculty of Engineering, Alexandria University. He is also serving as an Associate Editor of the IET Electric Power Applications Journal and as the Executive Editor of the Alexandria Engineering Journal. His current research interests include electrical machine design and modeling, electric drives, energy conversion and renewable energy.

Shehab Ahmed (SM'12) received his B.S. degree in Electrical Engineering from Alexandria University, Alexandria, Egypt, in 1999; and his M.S. and Ph.D. degrees from the Department of Electrical and Computer Engineering, Texas A&M University, College Station, TX, USA, in 2000 and 2007, respectively. He was with Schlumberger Technology Corporation, Houston, TX, USA, from 2001 to 2007, developing downhole mechatronic systems for oilfield service products. He was with the Texas A&M University at Qatar, Education City, Qatar, from 2007 to 2018 (currently on leave). He is presently working as a Professor of Electrical Engineering in the CEMSE Division at King Abdullah University of Science and Technology, Thuwal, Saudi Arabia. His current research interests include mechatronics, solid-state power conversion, electric machines and drives.